Toluene biodegradation in an algal-bacterial airlift photobioreactor: influence of the biomass concentration and the presence of an organic phase

Raquel Lebrero*, Roxana Ángeles, Rebeca Pérez, Raúl Muñoz

Department of Chemical Engineering and Environmental Technology, University of Valladolid, Dr. Mergelina, s/n, 47011, Valladolid, Spain. Tel. +34 983186424, Fax: +34983423013.

*Corresponding author: raquel.lebrero@iq.uva.es

Keywords: Airlift bioreactor, algal-bacterial photobioreactor, toluene biodegradation, two-phase partitioning bioreactor

Abstract

The potential of algal-bacterial symbiosis for off-gas abatement was investigated for the first time by comparatively evaluating the performance of a bacterial (CB) and an algal-bacterial (PB) airlift bioreactors during the treatment of a 6 g m^{-3} toluene laden air emission. The influence of biomass concentration and of the addition of a non-aqueous phase was also investigated. A poor and fluctuating performance was recorded during the initial stages of the experiment, which was attributed to the low biomass concentration present in both reactors and to the accumulation of toxic metabolites. In this sense, an increase in the dilution rate from 0.23 to 0.45 d^{-1} and in biomass concentration from ~1 to ~5 g L^{-1} resulted in elimination capacities (ECs) of 300 g m^{-3} h^{-1} (corresponding to removal efficiencies ~ 90 %). Microalgae activity allowed for a reduction in the emitted CO_2 and an increase in dissolved O_2 concentration in the PB. However, excess biomass growth over 11 g L^{-1} hindered light penetration and severely decreased photosynthetic activity. The addition of silicone oil at 20 % (on a volume basis) stabilized system performance, leading to dissolved O_2 concentrations of 7 mg L^{-1} and steady ECs of 320 g m^{-3} h^{-1} in the PB. The ECs here recorded were considerably higher than those previously reported in toluene-degrading bioreactors. Finally, microbial population analysis by DGGE-sequencing demonstrated the differential specialization of the microbial community in both reactors, likely resulting in different toluene degradation pathways and metabolite production.

1. Introduction

Due to its valuable psychoactive properties, the amount of toluene used in the chemical industry has noticeably increased over the last decades, leading to a concomitant increase in the atmospheric emissions of this aromatic pollutant (WHO 2000, EURAR-T 2003). Toluene causes toxic effects to both human health and the environment, and is considered a priority pollutant by the US-Environmental Protection Agency. Physical-chemical technologies for toluene removal, such as adsorption in activated carbon, thermal incineration or UV oxidation, generate hazardous by-products and/or wastes and entail high investment and operating costs. In this context, bioremediation based on bacterial or fungal activity has arisen as a cost-effective and environmentally sustainable alternative to conventional physical-chemical methods (Harding et al. 2003).

In particular, pneumatically agitated suspended-growth systems such as airlift bioreactors have demonstrated a cost-effective toluene abatement performance while avoiding typical operational problems encountered in packed-bed bioreactors: excessive biomass growth, flooding, channeling, pressure drop build-up or formation of anaerobic or dry zones (Vergara-Fdez et al. 2008). Nevertheless, airlift bioreactors for the treatment of toluene still face severe limitations such as (i) a limited pollutant mass transfer from the gas to the liquid phase due to its high Henry law, which results in a low pollutant bioavailability, (ii) microbial inhibition at high toluene inlet concentrations, and (iii) O_2 limitation when treating high toluene loads. An enhanced oxygen supply to the microbial community in the reactor by increasing the turbulence of the culture broth might be problematic since intensive mechanical aeration in bioreactors is highly costly and might cause volatilization and re-dispersion of the toluene present in the aqueous phase (Muñoz et al. 2005).

Photosynthetic oxygenation in algal-bacterial photobioreactors constitutes an efficient alternative to conventional aeration methods. In this process, the oxygen photosynthetically produced by microalgae in the presence of light and CO_2 is used by heterotrophic bacteria to *in situ* oxidize the organic pollutant, producing in return the CO_2 needed for microalgae photosynthesis. Unlike bacterial processes where the mineralization of organic pollutants releases CO_2 and H_2O as main end-products, microalgal processes are able to fix and recover carbon and other nutrients as valuable biomass besides furnishing O_2 to the heterotrophic community. Moreover, some microalgae are capable of biotransforming xenobiotic organic contaminants (Semple et al. 1999; Muñoz and Guieysse 2006). Therefore, microalgae may boost the biodegradation of toluene either by directly biotransforming the pollutant or by enhancing the degradation potential of the microbial community present in the bioreactor. Besides, additional O_2 supply by photosynthetic activity might prevent oxygen limitation and accelerate the bacterial degradation of toluene (Semple et al. 1999). Up to date, most studies on toluene biodegradation were based on the activity of bacteria and fungi. On the contrary, microalgae-supported biodegradation of aromatic contaminants has been scarcely investigated, and the catabolic pathways of biodegradation of aromatic compounds in microalgae are still largely unknown. Thus, despite the potential benefits of microalgae-based off-gas treatment, there is no single study comparatively evaluating the performance of algal-bacterial and bacterial bioreactors for the treatment of volatile organic compounds (VOCs).

On the other hand, the limited mass transfer of toluene to the liquid phase might be overcome by the addition to the bioreactor of a non-aqueous phase (NAP) with high affinity for this pollutant, resulting in a so-called two-liquid phase partitioning bioreactor (TLPPB). TLPPBs have been successfully applied to treat both high and low

VOC-laden gas emissions, improving the performance of biological processes (Muñoz et al. 2012, Lebrero et al. 2013). The NAP not only supports an enhanced mass transfer of the target pollutant and O_2 from the gas phase to the microorganisms, but also acts as a buffer against surges in pollutant or metabolite concentrations that might be potentially toxic to the microbial community (Lebrero et al. 2015).

This work was devised to comparatively evaluate a bacterial and an algal-bacterial airlift bioreactors treating toluene at high loading rates. The influence of biomass concentration and of the addition of a non-aqueous phase in order to overcome mass transfer limitations and the inhibition resulting from high toluene loads were also investigated. Moreover, the differential specialization of the microbial communities in both bioreactors was also assessed by molecular techniques.

2. Materials and Methods

2.1 Microorganisms and culture conditions

Both bioreactors were inoculated with a mixture of *Chlorella sorokiniana* (0.5 L), activated sludge from Valladolid wastewater treatment plant (0.1 L) and a toluene acclimated *Pseudomonas putida* DSM 6899 culture (0.35 L) to an initial total suspended solids concentration (TSS) of 0.79 g L^{-1}. The mineral salt medium (MSM) used throughout the entire experiment was composed of (g L^{-1}): KNO_3 1.25, $CaCl_2 \cdot H_2O$ 0.1105, H_3BO_3 0.1142, $FeSO_4 \cdot 7H_2O$ 0.0498, $ZnSO_4 \cdot 7H_2O$ 0.0882, $MnCl_2 \cdot 4H_2O$ 0.0144, MoO_3 0.0071, $CuCl_2 \cdot 2H_2O$ 0.0157, $CoCl_2 \cdot 2H_2O$ 0.0049, EDTA ($C_{10}H_{16}N_2O_8$) 0.5, KH_2PO_4 0.6247 and K_2HPO_4 1.3251.

2.2 Experimental set-up

The experimental plant consisted of two identical internal-loop airlift glass bioreactors with a total volume of 2.5 L and a working volume of 2.2 L, operated in parallel in an air-conditioned room at a constant temperature of 25 ºC (Figure 1). The inner tube had a diameter of 0.055 m and a height of 0.295 m, while the external cylinder diameter and height were 0.09 m and 0.42 m, respectively. A porous metallic diffuser, with an average pore diameter of 2 μm, was placed at the bottom of the inner tube to promote gas distribution. The air-lift photobioreactor (PB) was continuously illuminated with LED lamps arranged concentrically at an average intensity of 330.5 μmol m^{-2} s^{-1} (within the optimum range for the photosynthetic apparatus of microalgae, Muñoz and Guieysse 2006), while the control air-lift (CB) was covered with an opaque structure to prevent diffuse light penetration.

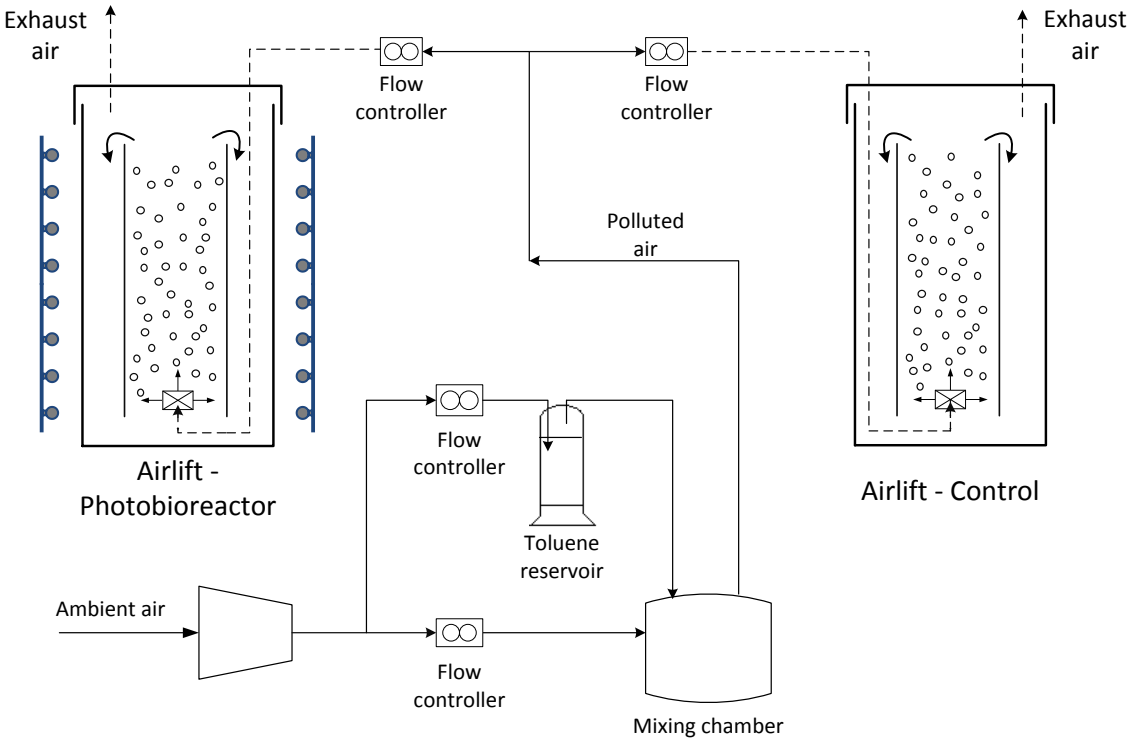

Figure 1. Schematic representation of the experimental set-up

The toluene-contaminated stream was obtained by sparging ambient air (flow controller, Aalborg, USA) in a reservoir containing liquid toluene kept at a constant temperature of 25 ± 2 ºC. The toluene-laden stream was then diluted with ambient air in a mixing chamber and subsequently divided into two identical streams (flow controller, Aalborg, USA) to feed both air-lift reactors. The toluene inlet concentration was maintained at 6.2 ± 0.7 g m^{-3} and the reactors were operated at an empty bed residence time of ~1.1 min (corresponding to an inlet load of 369 ± 45 g m^{-3} h^{-1}).

2.3 Operational procedure

During the first 6 days of operation, 0.5 L of the culture broth were daily removed from each bioreactor and replaced by fresh MSM. From day 6 to 26, the exchange of culture medium was increased to 1 L in order to avoid metabolite accumulation, which resulted in low TSS concentrations in both reactors. Therefore, 0.5 L of the 1L culture broth daily replaced were centrifuged and the biomass returned to the corresponding reactor from day 26 on. This strategy allowed controlling the biomass concentration and investigating the effect of this parameter on toluene removal performance. From day 46 onwards, the biomass recovered by centrifugation was increased to that corresponding to 0.9 L of the retrieved culture broth. Weekly cleanings were performed from day 14 to remove any biomass attached to the reactor walls. Finally, 20% of the culture broth was substituted by silicone oil 200 cSt (Sigma Aldrich, USA) at day 82 in order to improve process robustness.

Inlet and outlet gas concentrations of toluene and CO_2 were daily measured in both bioreactors. The pH, temperature and dissolved oxygen (DO) were daily recorded from the culture broths. Three times per week, samples from the culture broth were also taken to determine the concentration of TSS, total organic carbon (TOC) and total nitrogen

(TN) in both bioreactors. By day 68, samples from the liquid phase of each bioreactor were taken and analyzed in duplicate by SPME-GC-MS in order to assess the presence of any secondary metabolite accumulated in the culture broth.

Finally, six samples for microbial analysis were collected and stored immediately at −20°C. Samples 1 and 2 corresponded to the CB and the PB inoculum, respectively. The rest of the samples were retrieved at the end of the experiment (day 106) from the suspended biomass in the CB (sample 3) and the PB (sample 4), and from the biomass attached to the reactor walls in the CB (sample 5) and the PB (sample 6).

2.4 Analytical methods

Toluene gas concentration was measured using a Varian 3900 gas chromatograph (Palo Alto, USA) equipped with a flame ionization detector and a SupelcoWax capillary column (15 m × 0.25 mm × 0.25 μm). The injector, detector and oven temperatures were set at 210, 250 and 140 ºC, respectively. CO_2 concentration was determined in a Bruker 430 gas chromatograph (Palo Alto, USA) coupled with a thermal conductivity detector and equipped with a CP-Molsieve 5A (15 m × 0.53 μm × 15 μm) and a CP-Pora-BOND Q (25 m × 0.53 μm × 10 μm) columns. The oven, injector and detector temperatures were maintained at 45, 150 and 175ºC, respectively.

Temperature and DO concentration in the culture broth of both reactors were monitored by an OXI 330i oximeter (WTW, Germany). The pH of the liquid samples was determined by a pH meter Crison 50 12T (Crison Instruments, Spain), while biomass concentration was measured as TSS according to Standard Methods (American Water Works Association, 2012). Samples for the determination of TOC and TN concentrations were filtered through 0.22 μm filters (Merck Millipore, USA) prior to

analysis in a TOC-VCSH analyzer (Shimadzu, Japan) coupled with a chemiluminescense detection TN module (TNM-1) (Shimadzu, Japan).

The presence of secondary metabolites in the culture broth was analyzed as follows: 1.7-mL glass vials were filled with 1.5 mL of the culture broth sample and closed with Teflon/rubber caps. Samples were pre-concentrated by SPME by immersing an 85-μm Carboxen/PDMS fibre (Supelco, Bellefonte, USA) into the leachate for 5 min. The SPME fibre was then injected and allowed to desorb for 1 min in an Agilent 6890N GC–MS equipped with a DB-WAX column (30 m × 0.250 mm × 0.25 μm) (J&W Scientific®, CA, USA). The injector temperature was set at 200 °C while the oven temperature was initially maintained at 40 °C for 4 min and then increased at 10 °C min^{-1} up to 200 °C. Source and MS quadrupole temperatures were set at 230 and 150 °C, respectively. Only compounds with a match quality ≥ 90 % were considered in the discussion.

2.5 Microbiological procedures

Genomic DNA was extracted using the protocol described in the Fast® DNA Spin Kit for Soil (MP Biomedicals, LLC) handbook. The V6–V8 region of the bacterial 16S rRNA genes was amplified by polymerase chain reaction (PCR) using the universal bacterial primers 968-F-GC and 1401-R (Sigma–Aldrich, St. Louis, MO, USA). The PCR mixture contained 1 μL of each primer (10 ng μL^{-1} each primer), 25 μL of BIOMIX ready-to-use 2 reaction mix (Bioline, Ecogen), 2 μL of the extracted DNA, and Milli-Q water up to a final volume of 50 μL. The PCR thermo-cycling program consisted of 2 min of pre-denaturation at 95°C, 35 cycles of denaturation at 95°C for 30

s, annealing at 56°C for 45 s, and elongation at 72°C for 1 min, with a final 5-min elongation at 72°C.

The DGGE analysis of the amplicons was performed with a D-Code Universal Mutation Detection System (Bio Rad Laboratories) using 8 % (w/v) polyacrylamide gels with a urea/formamide denaturing gradient of 45 to 65 %. DGGE running conditions were applied according to Roest et al. (2005). The gels were stained with GelRed Nucleic Acid Gel Stain (biotium) for 1 h. The most relevant bands were excised from the DGGE gel in order to identify the bacteria present in the samples, resuspended in 50 µL of ultrapure water and maintained at 60 °C for 1 h to allow DNA extraction from the gel. A volume of 5 µL of the supernatant was used for reamplification with the original primer set. Before sequencing, PCR products were purified with the GenElute PCR DNA Purification Kit (Sigma-Aldrich, St. Louis, MO, USA).

DGGE profiles were compared using the GelCompar IITM software (Applied Maths BVBA, Sint-Martens-Latem, Belgium). After image normalization, bands were defined for each sample using the bands search algorithm within the program. The peak heights in the densitometric curves were also used to determine the diversity indices based on the Shannon–Wiener diversity index (H), calculated as follows:

$$H = -\sum \left[P_i \ln(P_i) \right]$$

where H is the diversity index and Pi is the importance probability of the bands in a lane (Pi = n_i/n, where n_i is the height of an individual peak and n is the sum of all peak heights in the densitometric curves). Therefore, this index reflects both the sample richness (relative number of DGGE bands) and evenness (relative intensity of every band).

Similarity indices of the compared samples were calculated from the densitometric curves of the scanned DGGE profiles by using the Pearson product–moment correlation coefficient (Häne et al. 1993). The taxonomic position of the sequenced DGGE bands was obtained using the RDP classifier tool (50% confidence level) (Wang et al. 2007). The closest cultured and uncultured relatives to each band were obtained using the BLAST search tool at the NCBI (National Centre for Biotechnology Information) (McGinnis and Madden 2004). The sequences generated from this work are deposited in GenBank under accession numbers KT200332-KT200347.

3. Results and Discussion

3.1. Bacterial and algal-bacterial airlifts performance

A different performance was observed during the start-up of both bioreactors despite following the same inoculation procedure. Whereas toluene removal efficiency (RE) peaked at 99 % immediately after start-up in the control bioreactor, decreasing afterwards to ~16 % by day 5, a maximum RE of 50 % was recorded by day 3 of operation in the photobioreactor, gradually decreasing to zero by day 5 (Figures 2a and 2b). The MSM renewal rate was then doubled by day 6 to 1 L day^{-1} (corresponding to a dilution rate of 0.45 d^{-1}) and maintained during the second operational stage. However, a consistent low toluene biodegradation performance was recorded in both bioreactors in spite of the higher MSM replacement rate until periodic reactor walls cleanings were initiated. Biomass detachment allowed for a slight increase in the suspended biomass concentration and consequently in the abatement performance recorded in stage II. In this sense, toluene REs fluctuated from 17 to 90 % in the PB and from 58 to 87 % in the CB between days 15 and 26, the maximum elimination capacities (ECs) being recorded immediately after biomass detachment from the reactor walls in both systems (Figures 2

and 3). During these first and second operational stages, biomass concentration increased from 0.8 g L^{-1} to 4 g L^{-1} in the PB and to 2.2 g L^{-1} in the CB as a result of an enhanced toluene degradation (Figure 4).

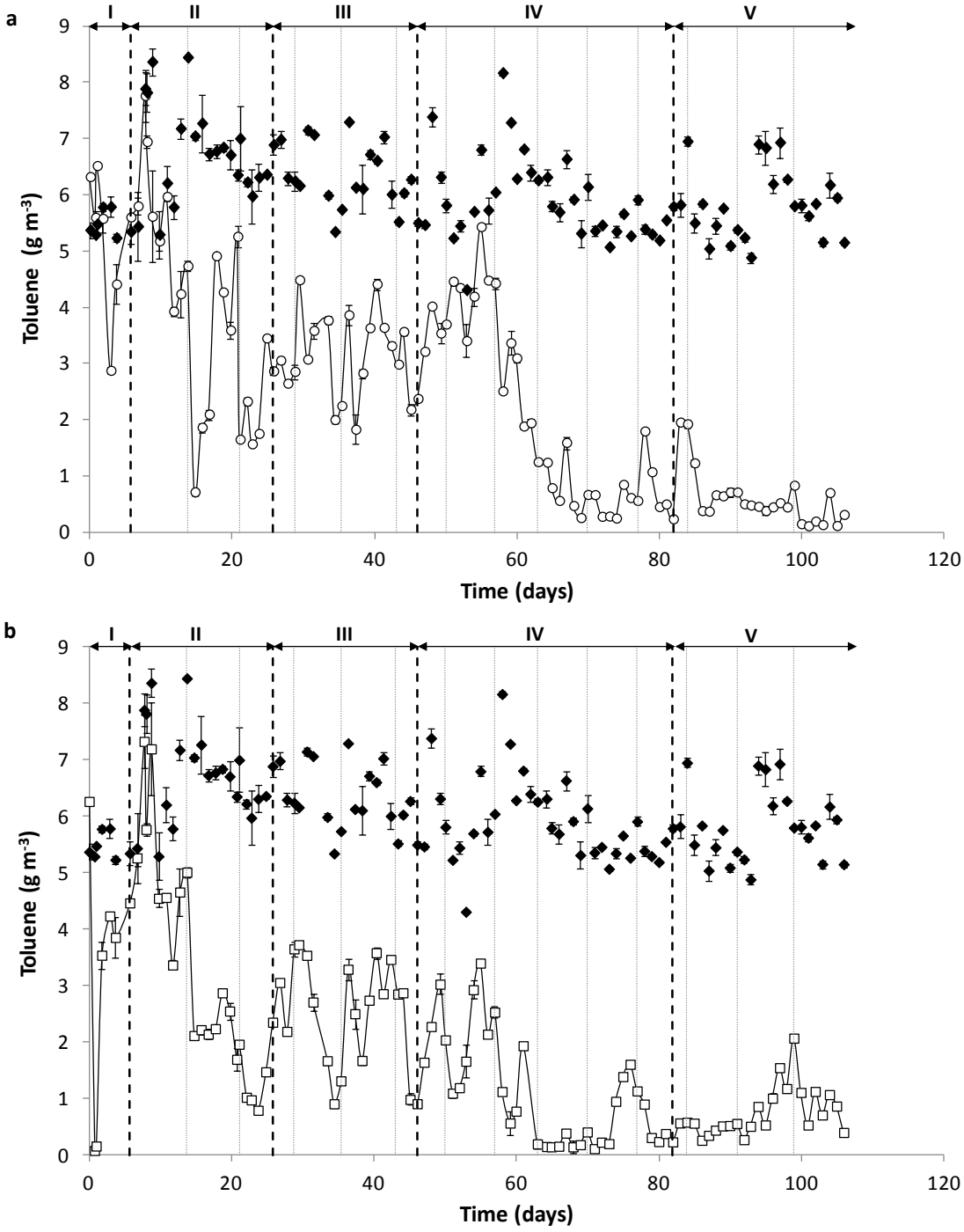

Figure 2. Time course of toluene inlet (♦) and outlet concentration in (a) the photobioreactor (○) and (b) control reactor (□) operated at an empty bed residence time of 1.1 min. Dotted lines represent the reactor cleanings and dashed lines the different operating stages as indicated in the upper part of each graph.

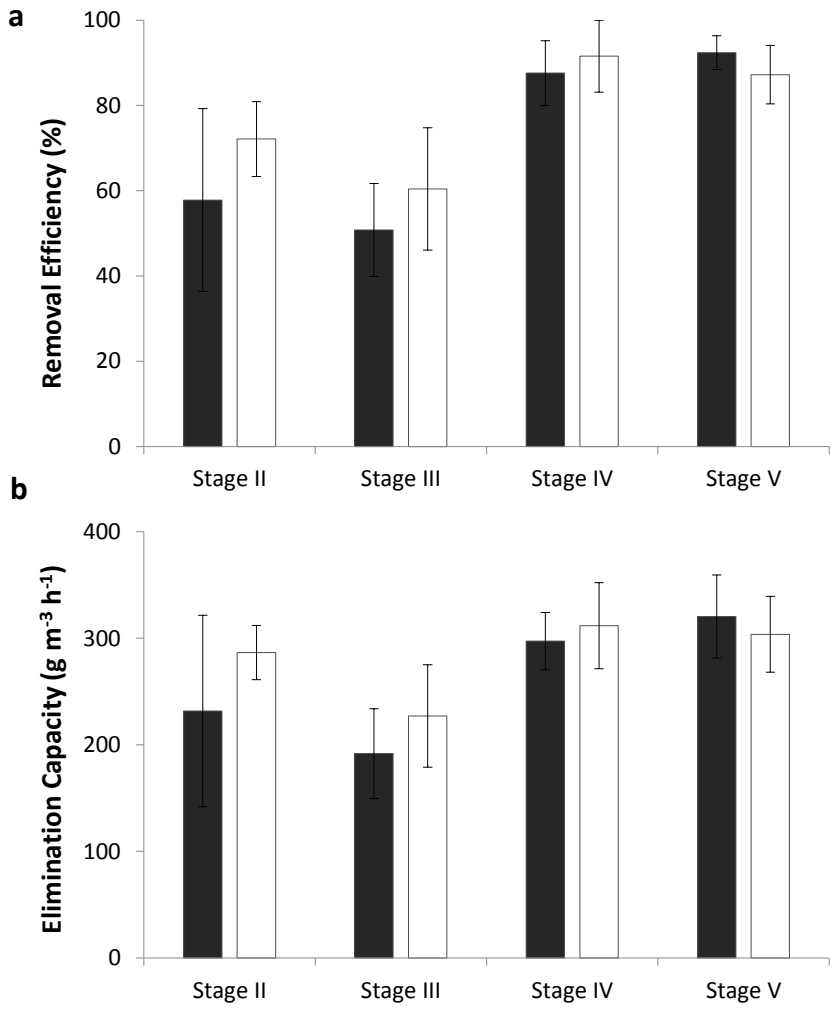

Figure 3. Average removal efficiency (a) and elimination capacity (b) recorded in the photobioreactor (black columns) and control airlift reactor (white columns) in the different operating stages. Vertical bars represent standard deviations.

The concentration of CO_2 also increased concomitantly with toluene removal, with average values (days 20-25) of 14.0 ± 0.6 g m^{-3} in the CB and of 3.1 ± 0.8 g m^{-3} in the PB. These lower CO_2 emissions in the PB confirmed the intense photosynthetic activity (Figure 5a). The dissolved O_2 concentration recorded during stage II was also higher in the PB (5.9 ± 0.8 mg L^{-1}) than in the CB (0.4 ± 0.1 mg L^{-1}) as a result of microalgal photosynthesis (Figure 5b). The unstable performance observed in both reactors during stage II (days 5-26) was attributed to the inhibition of microbial activity mediated by the accumulation of toxic metabolites and to the progressive accumulation of biomass in the

reactor walls, resulting in a low suspended biomass concentration. In this sense, biomass detachment from the reactor walls led to a higher suspended biomass concentration, which entailed a one-off increase in the removal efficiency. This increase in toluene removal resulted in higher metabolites concentrations and therefore in a subsequent decrease in the reactor performance, which was again restored after the following cleaning. Nevertheless, along this second stage, biomass accumulation globally resulted in higher toluene REs. Several authors have previously highlighted the key role of biomass concentration and metabolites accumulation on microbial instability in bioprocesses treating toluene (Bordel et al. 2007, Díaz et al. 2008). In this context, Díaz et al. (2008) observed that restoration of system performance after the accumulation of inhibitory metabolites in a suspended growth reactor treating toluene was not immediate likely due to the deterioration of the toluene degrading community.

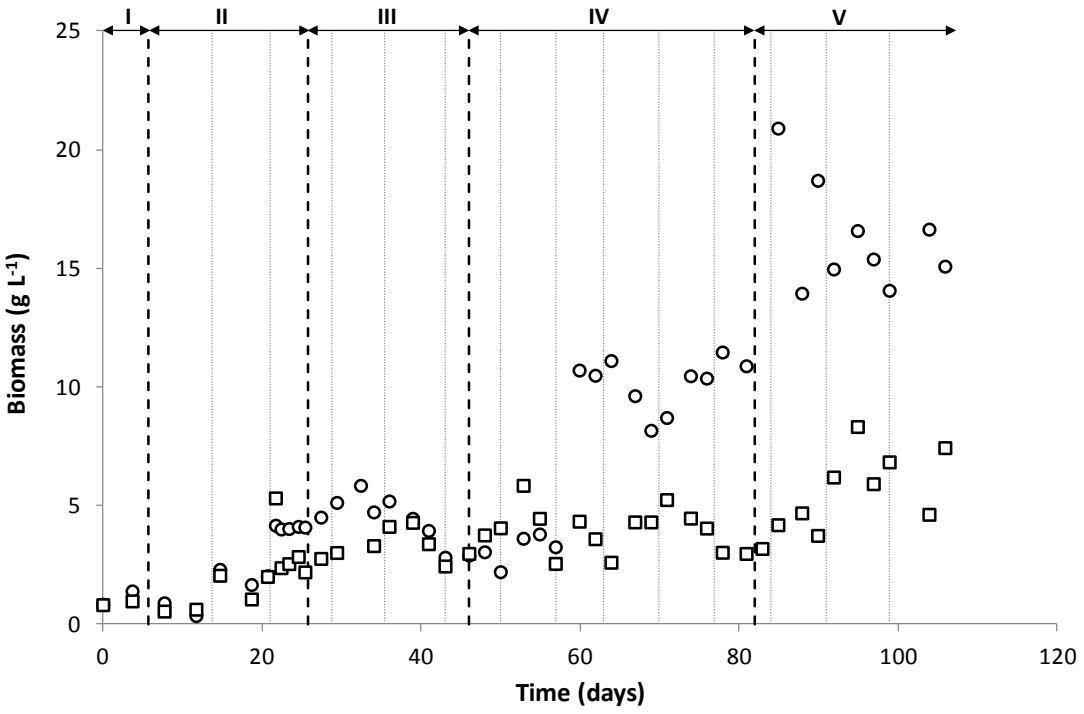

Figure 4. Time course of the biomass concentration as total suspended solids concentration in the photobioreactor (○) and control reactor (□). Dotted lines represent the reactor cleanings and dashed lines the different operating stages as indicated in the upper part of each graph.

At this point, it was evident that microbial activity was limiting toluene abatement in both bioreactor configurations. Thus, half of the exchanged media was daily centrifuged and the biomass returned to the corresponding reactor during stage III in order to further increase the suspended solids concentration in the reactors. This operational strategy initially resulted in a TSS increase up to 5.8 and 4.3 g L^{-1} in the PB and CB, respectively, both concentrations stabilizing at ~2.9 g L^{-1} by day 46 (Figure 4). During this stage, average toluene removals of 51 ± 11% in the PB and 60 ± 14% in the CB were recorded. Despite the enhancement in toluene abatement mediated by the increase in biomass concentration, both bioreactors still exhibited a highly fluctuating performance (Figures 2 and 3). A lower CO_2 concentration was also recorded along stage III in the PB compared to that of the CB, although a gradual decrease in the photosynthetic activity was observed from day 37. This deterioration in microalgae activity resulted in higher CO_2 outlet concentrations and lower dissolved oxygen values in the PB (9.1 ± 0.9 g m^{-3} and 0.2 ± 0.1 mg L^{-1}, respectively) (Figure 5). Unfortunately, this behavior could not be attributed to any macroscopic change in the photobioreactor.

From day 46 onwards (stage IV), 90 % of the retrieved culture broth was centrifuged in order to recover and return the biomass to both bioreactors. While this procedure resulted in a significant biomass accumulation in the photobioreactor (10.2 ± 1.1 g L^{-1} by day 60), the TSS value remained at 3.9 ± 0.8 g L^{-1} in the control airlift (Figure 4). Stabilization in the abatement performance at REs of 87.6 ± 7.6 % and 91.6 ± 8.4 % was observed from day 63 onwards in the PB and the CB, respectively, corresponding to ECs of 297.1 ± 26.9 and 311.7 ± 40.4 g m^{-3} h^{-1}. These high toluene removals resulted in a decrease in the DO values in both reactors. Under these operational conditions, photosynthetic activity in the PB was severely deteriorated as shown by the outlet CO_2 concentrations in the PB (16.5 ± 2.4 g m^{-3}) compared to those recorded in the CB (20.1

± 2.1 g m^{-3}) under comparable REs. At this point, it is important to stress that biomass concentration in the PB is not only a key parameter governing pollutant removal rate, but also determining the light utilization efficiency by microalgae. In this sense, no further increase in photosynthetic oxygenation rate occurs above a critical biomass concentration due to mutual shading and algal dark respiration as demonstrated by Muñoz et al. (2004). This deterioration in photosynthetic activity was correlated to the increase in biomass concentration in the PB by day 60, which likely hindered light penetration with the concomitant reduction in microalgae CO_2-fixation capacity.

In order to identify the different metabolites present in the culture broth, samples from the liquid phase of each bioreactor were taken at day 68 and analyzed in duplicate by SPME-GC-MS. Despite the limitation of this technique due to the hydrophobic nature of the PDMS fibre (which only allowed the detection of non-water soluble compounds), significant differences were observed between both culture broths. For instance, among the aromatic and alcohol derivative compounds detected, oxyme- methoxy- phenyl benzene was retrieved from both samples, while 1,2 benzene dicarboxylic acid was only found in the CB and 2- (2-ethoxyethoxy) ethanol was the most significant metabolite in the PB. α-dimethylamino 4-ethoxy o-cresol was only detected in the photobioreactor airlift. These results suggested the occurrence of different toluene degradation pathways depending on the microbial community, thus resulting in the accumulation of different extracellular metabolites.

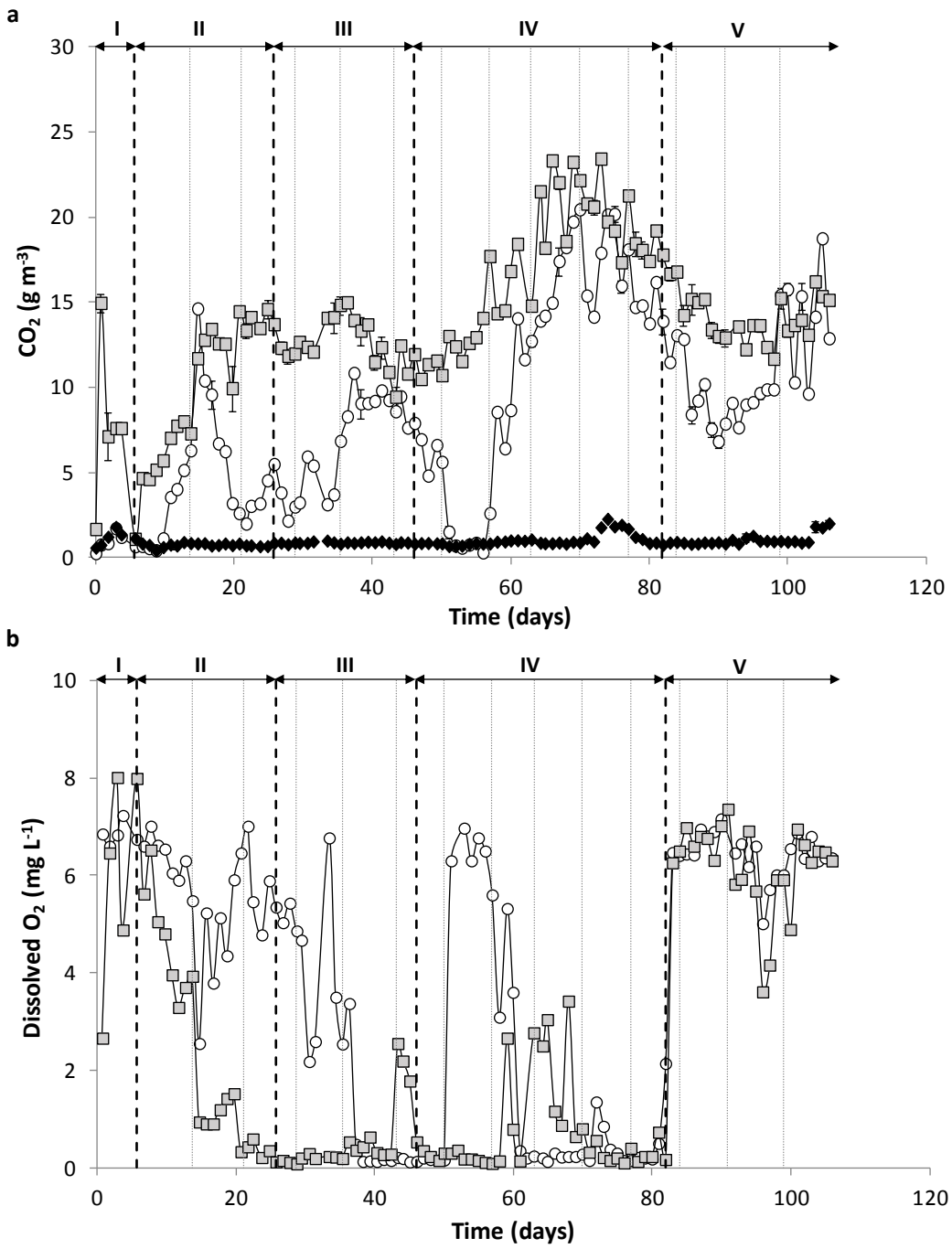

Figure 5. Time course of (a) CO_2 inlet (♦) and outlet concentration in the photobioreactor (○) and control reactor (□); (b) dissolved oxygen concentration in the photobioreactor (○) and control reactor (□). Dotted lines represent the reactor cleanings and dashed lines the different operating stages as indicated in the upper part of each graph.

Finally, the addition of silicone oil supported an increase in the DO concentration in both reactors (Figure 5b). The removal performance of the photobioreactor experienced both a slight increase and a stabilization at 92.4 ± 4.0 % (EC = 320.4 ± 38.9 g m^{-3} h^{-1}),

while biomass accumulated up to ~15 g L^{-1}. Steady REs (except for a sudden decrease by day 99) of 87.2 ± 6.9 % were recorded in the control airlift during this last stage (corresponding to an EC = 303.6 ± 35.6 g m^{-3} h^{-1}), together with an increase in biomass concentration up to 5.6 ± 2.7 g L^{-1}. Several authors have demonstrated a mass transfer enhancement of poorly water soluble compounds (as is the case of toluene and oxygen, with Henry constants H=Ca/Cg of 3.7 and 0.03, respectively (Sander 2014)) when a non-aqueous phase such as silicone oil is added to the bioreactor. This enhanced toluene mass transfer was not only related with the higher solubility of the toluene in the silicone oil, but also with an enhanced gas/water interfacial area (Quijano et al. 2010, Lebrero et al. 2013). Moreover, the addition of this non-aqueous phase to the bioreactors acted as a metabolite reservoir, thus avoiding inhibitory concentrations in the culture broth.

The ECs here recorded were considerably higher than those reported in toluene-degrading biofilters, ranging from 90 up to 165 g m^{-3} h^{-1} at toluene inlet concentrations of 0.4-8 g m^{-3} (Jorio et al. 1998, Singh et al. 2010, Gallastegui et al. 2013, Cheng et al. 2016). These ECs were also higher than previous experiments performed in airlift bioreactors. Vergara-Fernandez et al. (2008) reported maximum ECs of 230 g m^{-3} h^{-1} at ~8 g m^{-3} of toluene, while Harding et al. (2003) only achieved 35 g m^{-3} h^{-1} in an external loop airlift fed with 15 g m^{-3} of toluene. Airlift bioreactors are a cost-effective alternative for the implementation of aerobic off-gas treatment processes compared to packed-bed bioreactors, besides providing a better process control. The high toluene removal performance here achieved, together with its inherently low energy consumption, support the applicability of this pneumatically aerated configuration. Moreover, the presence of a microalgae community in the PB showed a beneficial effect during stage II by reducing the amount of CO_2 emitted to the atmosphere compared to

that of the CB concomitantly with an increase in the DO concentration in the cultivation media. Finally, the operation of the airlift as a two-phase partitioning reactor with the addition of silicone oil further enhanced not only toluene but also oxygen mass transfer, thus preventing O_2 limiting scenarios.

3.2 Microbial analysis

The Shannon-Wiener diversity indices obtained showed that the high diversity of the inoculum was maintained throughout the experiment despite the selective pressure of toluene and its metabolites (Figure 6). This diversity index, with typical values ranging from 1.5 to 3.5 (low and high species evenness and richness, respectively) (McDonald 2003) was similar for all the samples retrieved, varying from 2.33 (biomass attached onto the PB) to a highest value of 2.94 corresponding to the inoculum and the biomass attached in the CB. As expected, a low Pearson similarity value of 32.4 % was recorded between the suspended biomass samples of both bioreactors, although the attached biomass retrieved from the CB and the PB showed a similarity of 74.9 %.

From the DGGE gel, 16 bands were sequenced (Figure 6, Table 1), rendering six different phyla: *Proteobacteria* (eight bands), *Acidobacteria* (four bands), *Cyanobacteria/Chloroplast* (one band), *Ignavibacteriae* (one band), *Actinobacteria* (one band) and *Chloroflexi* (one band). The closest cultured and uncultured relatives of each band were determined by NCBI BLAST analysis and summarized in Table 1 along with the environment from which the closest organisms were retrieved. The VOC biodegradation capacity of some of the microorganisms here identified has been already reported in the literature. For instance, from the bands retrieved in both bioreactors, bacteria from the genus *Xanthobacter flavus* (band 7) and *Bryobacter* (band 11) within the phylum *Proteobacteria* are able to degrade phenol (Nagamani et al. 2009), while

members of the family *Enterobacteriaceae* (band 8) have been found to transform aromatics under both aerobic and anaerobic conditions, tolerating and removing different polycyclic aromatic hydrocarbons (Toledo et al. 2006). Microorganisms from the genus *Ignavibacterium* (phylum *Ignavibacteriae*) (band 14) and from the phylum *Chloroflexi* (band 16) have been also retrieved from toluene treatment systems (Lebrero et al. 2012, Kuppardt et al. 2014). Six of the DGGE sequenced fragments were only found in the CB (1, 3, 5, 6, 12 and 15), from which bands 6 (order *Rhizospirales*, phylum *Proteobacteria*) and 15 (genus *Mycobacterium*, phylum *Actinobacteria*) were also identified as PAH and BTEX degrading microorganisms, respectively (Martin et al. 2012, Zhang et al. 2013). Finally, DGGE fragments 9, 10 and 13 were only retrieved from the PB. In particular, band 13 was identified as *Chlorella Sorokiniana*, with a higher relative abundance in the suspended biomass sample. *Blastocatella*-like bacteria (bands 9 and 10), commonly found in biological systems treating petrochemical effluents, likely played a key role in toluene degradation in the photobioreactor based on the intensity of the DGGE bands (Yang et al. 2015, Fu et al. 2016).

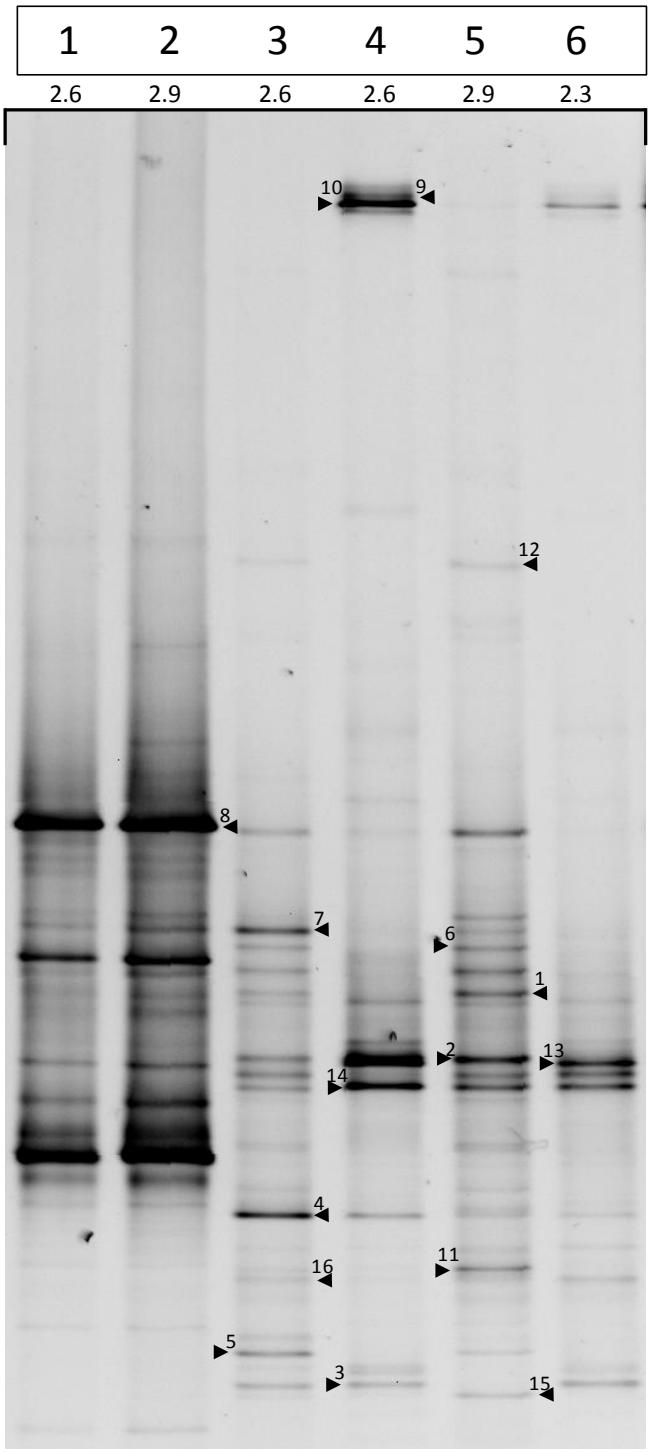

Figure 6. DGGE profile of the main bacterial communities present in the CB inoculum (1), PB inoculum (2), suspended biomass at day 106 in the CB (3) and the PB (4), and attached biomass at day 106 in the CB (5) and PB (6). The Shannon-Wiener diversity indexes are indicated in the upper part of the gel. The sequenced bands are indicated by "►'' and the corresponding number of each band.

Table 1. RDP classification of the DGGE bands sequenced and corresponding matches (BLASTN) using the NCBI database with indication of the similarity percentages and sources of origin. The presence/absence of each band in each sample tested together with its intensity are also shown.

Taxonomic placement (50% confidence level)	Band n°	1	2	3	4	5	6	Closest relatives in Blast Name (accession number)	Similarity (%)	Source of origin
Phylum *Proteobacteria*	1	x	xx	xx		xx		Uncultured *delta proteobacterium* (JN038629)	89	Soil
Class *Alphaproteobacteria*	2			xx	xxx	xxx	xx	Uncultured bacterium (JQ072580)	90	Brewery wastewater pilot reactor
Order *Rhodospirillales*										
Family *Rhodospirillaceae*	3			x	x	xx		Bacterium (AB208736)	96	Culture collection
Genus *Azospirillum*	4			xxx	xx	x	x	*Azospirillum fermentarium* (NR_118484)	99	Nitrogen-fixing species
								Uncultured bacterium (JX174657)	97	Microbial fuel cell fed with olive mill wastewater as sole carbon source
	5			xx		x		*Azospirillum sp.*(HQ694759)	99	Autotrophic enrichment culture En_UW_28 with $Na_2S_2O_3$ as electron donor
								Azospirillum brasilense (FR667883)	99	Culture collection
								Azospirillum sp. (AY061963)	99	Culture collection
Order *Rhizospirales*	6			xx		xx		Uncultured bacterium (FQ659151)	90	PAH degrading bacterial community in contaminated soil
Family *Xanthobacteraceae*										
Genus *Xanthobacter*	7	x	xx	xxx	x	xx	x	*Xanthobacter sp.*(HF566355)	99	Vineyard soil
								Xanthobacter flavus (AB512110)	99	Polyvinyl alcohol-degrading bacteria from activated sludge
Class *Gammaproteobacteria*										
Order *Enterobacteriales*										
Family *Enterobacteriaceae*	8	xxx	xxx	xx	x	xx		*Erwinia sp.* (KF999718)	99	Extraction of Luffa cylindrica fruits
Phylum *Acidobacteria*										
Class *Acidobacteria_Gp4*										
Genus Blastocatella	9				xxx		x	Uncultured bacterium (JX394456)	98	Aerosol microbiology in a metropolitan subway system
								Uncultured bacterium (DQ984629)	98	Oil-contaminated soil
	10				xxx	x	xx	Uncultured bacterium (JN603801)	98	Rhizosphere soil from field grown riceplants
								Uncultured bacterium (DQ984629)	98	Oil-contaminated soil
Class *Acidobacteria_Gp3*										
Genus Bryobacter	11	x	x	x	x	xx		Uncultured bacterium (FQ659827)	97	PAH degrading bacterial community of a contaminated soil
								Uncultured bacterium (EF393024)	97	Anaerobic polychlorinated biphenyl dechlorinating consortia
Class *Holophagae*										
Order *Holophagales*										
Family *Halophagaceae*										
Genus *Geothrix*	12			x		x		Uncultured bacterium (KC758898)	98	Sulfate-reducing MTBE and TBA plume

								Uncultured *Geothrix sp*. (AJ583203)	98	Ground water from a monitoring deep-well at a radioactive waste disposal site
								Uncultured bacterium (JQ996662)	98	Activated sludge in an anaerobic methane oxidation reactor
Phylum *Cyanobacteria/Chloroplast*										
Class *Cloroplast*										
Family *Chloroplast*										
Genus *Chlorophyta*	13	xx	xx		xxx		xxx	*Chlorella sorokiniana* (KF981992)	99	Water
								Chlorella sorokiniana (KJ742376)	99	Culture collection
								Chlorella sp. (KM218897)	99	Coastal water
								Uncultured *Chlorella* (KC994689)	97	Microalgae photobioreactor
Phylum *Ignavibacteriae*										
Class *Ignavibacteria*										
Order *Ignavibacteriales*										
Family Ignavibacteriaceae										
Genus *Ignavibacterium*	14			xx	xxx	xxx	xxx	Uncultured bacterium (JX040332)	99	Waste water
								Uncultured sludge bacterium (FJ947134)	98	Activated sludge in a livestock wastewater treatment plant
								Uncultured bacterium (JQ624282)	98	Wastewater treatment plant
Phylum *Actinobacteria*										
Class *Actinobacteria*										
Subclass *actinobacteridae*										
Order *actinomycetales*										
Suborder *Corynebacterineae*										
Family *Mycobacteriaceae*										
Genus *Mycobacterium*	15	x	x		x			*Mycobacterium sp*.(KJ729254)	99	Activated sludge from wastewater treatment plant
								Uncultured bacterium (HE965750)	99	PAH-degrading bacteria isolated from oil-containing sewage soil
								Mycobacterium gilvum (JN590246)	99	Oil-containing sewage soil
Phylum *Chloroflexi*	16			x	x	x	x	Uncultured *Chloroflexi bacterium* (FJ912105)	91	Marine sediment

4. Conclusions

This study confirmed the superior performance of bacterial and algal-bacterial airlift reactors over conventional biofilters for the removal of toluene, which achieved ECs up to 320 g m^{-3} h^{-1} at empty bed residence times of 1.1 min. Biomass concentration and medium renewal rate played a key role on toluene abatement performance, with optimum values of ~5 g L^{-1} and 0.45 d^{-1} (with a 90% biomass recycling), respectively. Moreover, photosynthetic activity in the photobioreactor resulted in lower emissions of CO_2 and higher dissolved oxygen concentrations when suspended biomass was maintained below 5 g L^{-1}, with higher values leading to mutual shading and therefore a low photosynthetic efficiency. The results also showed the positive impact of silicone oil addition on the stabilization of toluene biodegradation due to an enhanced O_2 mass transfer and buffering against toxic metabolites. Finally, the presence of microalgae in the PB induced the enrichment of a microbial community different than that stablished in the CB, as suggested by the low similarity observed between the microbial communities identified by the end of the operation and between the metabolites detected in the culture broth of both bioreactors.

Acknowledgments

This research was supported by MINECO (CTM2015-70442-R and Red Novedar) and the Regional Government of Castilla y León (Project VA024U14 and UIC 71). CONACyT-México is also gratefully acknowledged for the Master grant of Roxana Angeles.

References

American Water Works Association (2012) Standard methods for the examination of water and wastewater. American Water Works Association 1469.

Bordel S., Muñoz R., Díaz L.F. and Villaverde S. (2007) Predicting the accumulation of harmful metabolic byproducts during the treatment of VOC emissions in suspended growth bioreactors. Environmental Science and Technology 41, 5875-5881.

Cheng Z., Lu L., Kennes C., Yu J. and Chen J. (2016) Treatment of gaseous toluene in three biofilters inoculated with fungi/bacteria: Microbial analysis, performance and starvation response. Journal of Hazardous Materials 303, 83-93.

Díaz L.F., Muñoz R., Bordel S. and Villaverde S. (2008) Toluene biodegradation by Pseudomonas putida F1: targeting culture stability in long-term operation. Biodegradation 19, 197-208.

EURAR-T, 2003. European Union Risk Assessment Report –Toluene (EINECS No. 203-625-9), vol. 9, PL2.

Fu L.Y., Wu C.Y., Zhou Y.X., Zuo J.E. and Ding Y. (2016) Treatment of petrochemical secondary effluent by an up-flow biological aerated filter (BAF). Water Science and Technology, in press.

Gallastegui G., Barona A., Rojo N., Gurtubay L. and Elías A. (2013) Comparative response of two organic biofilters treating ethylbenzene and toluene after prolonged exposure. Process Safety and Environmental Protection 91, 112-122.

Häne B.G., Jäger K. and Drexler H.G. (1993) The Pearson product-moment correlation coefficient is better suited for identification of DNA fingerprint profiles than band matching algorithms. Electrophoresis 14, 967–972.

Harding R.C., Hill G.A. and Lin Y.H. (2003) Bioremediation of toluene-contaminated air using an external loop airlift bioreactor. Journal of Chemical Technology and Biotechnology 78, 406-411.

Jorio H., Kiared K., Brzezinski R., Leroux A., Viel G. and Heitz M. (1998) Treatment of air polluted with high concentrations of toluene and xylene in a pilot-scale biofilter. Journal of Chemical Technology and Biotechnology 73, 183-196.

Kuppardt A., Kleinsteuber S., Vogt C., Lüders T., Harms H. and Chatzinotas A. (2014) Phylogenetic and functional diversity within toluene degrading, sulphate reducing consortia enriched from a contaminated aquifer. Microbial Ecology 68, 222-234.

Lebrero R., Rodríguez E., Estrada J.M., García-Encina P.A. and Muñoz R. (2012) Odor abatement in biotrickling filters: Effect of the EBRT on methyl mercaptan and hydrophobic VOCs removal. Bioresource Technology 109, 38-45.

Lebrero R., Rodríguez E., Pérez R., García-Encina P.A. and Muñoz R. (2013) Abatement of odorant compounds in one- and two-phase biotrickling filters under steady and transient conditions. Applied Microbiology and Biotechnology 97, 4627-4638.

Lebrero R., Hernández R., Pérez R., Estrada J.M. and Muñoz R. (2015) Two-liquid phase partitioning biotrickling filters for methane abatement: Exploring the potential of hydrophobic methanotrophs. Journal of Environmental Management 151, 124-131.

McDonald G (2003) Biogeography: space, time and life. Wiley, New York, p 409

McGinnis S. and Madden T.L. (2004) BLAST: at the core of a powerful and diverse set of sequence analysis tools. Nucleic Acids Research 32, W20–25.

Martin F., Torelli S., Le Paslier D., Barbance A., Martin-Laurent F., Bru D., Geremia R., Blake G. and Jouanneau Y. (2012) Betaproteobacteria dominance and diversity shifts in the bacterial community of a PAH-contaminated soil exposed to phenanthrene. Environmental Pollution 162, 345-353.

Muñoz R., Köllner C., Guieysse B. and Mattiasson B. (2004) Photosynthetically oxygenated salicylate biodegradation in a continuous stirred tank photobioreactor. Biotechnology Bioengineering 87, 797–803.

Muñoz R., Rolvering C., Guieysse B. and Mattiasson B. (2005) Photosynthetically oxygenated acetonitrile biodegradation by an algal-bacterial microcosm: a pilot-scale study. Water Science and Technology 51, 261-265.

Muñoz R. and Guieysse B. (2006) Algal-bacterial processes for the treatment of hazardous contaminants: A review. Water Research 40, 2799-2815.

Muñoz R., Daugulis A.J., Hernández M. and Quijano G. (2012) Recent advances in two phase partitioning bioreactors for the treatment of volatile organic compounds, Biotechnology Advances 30, 1707–1720.

Nagamani A., Soligalla R. and Lowry M. (2009) Isolation and characterization of phenol degrading Xanthobacter flavus. Bioremediation Journal 13, 1-6.

Quijano G., Rocha-Rios J., Hernández M., Villaverde S., Revah S., Muñoz R. and Thalasso F. (2010). Determining the effect of solid and liquid vectors on the gaseous interfacial area and oxygen transfer rates in two-phase partitioning bioreactors. Journal of Hazardous Materials 175, 1085-1089.

Roest K, Heilig H.G., Smidt H., de Vos W.M., Stams A.J.M. and Akkermans A.D.L. (2005) Community analysis of a full-scale anaerobic bioreactor treating paper mill wastewater. Systematic and Applied Microbiology 28, 175– 185.

Sander R. (2014) Compilation of Henry's law constants, version 3.99. Atmospheric Chemistry and Physics Discussions 14, 29615-30521.

Semple K.T., Cain R.B. and Schmidt S. (1999) Biodegradation of aromatic compounds by microalgae. FEMS Microbiology Letters 170, 291-300.

Singh R.S., Rai B.N. and Upadhyay S.N. (2010) Removal of toluene vapour from air stream using a biofilter packed with polyurethane foam. Process Safety and Environmental Protection 88, 366-371.

Toledo F.L., Calvo C., Rodelas B. and González-López J. (2006) Selection and identification of bacteria isolated from waste crude oil with polycyclic aromatic hydrocarbons removal capacities. Systematic and Applied Microbiology 29, 244-252.

Vergara-Fernández A.O., Quiroz E.F., Aroca G.E. and Pulido N.A. (2008) Biological treatment of contaminated air with toluene in an airlift reactor. Electronic Journal of Biotechnology 11, 1-7.

Wang Q., Garrity G.M., Tiedje J.M. and Cole J.R. (2007) Naive Bayesian classifier for rapid assignment of rRNA sequences into the new bacterial taxonomy. Applied and Environmental Microbiology 73, 5261–5267.

WHO (2000) Air Quality Guidelines, Regional Office for Europe, Denmark. Second Edition, Chapter 5.14

Yang Q., Xiong P., Ding P., Chu L. and Wang J. (2015) Treatment of petrochemical wastewater by microaerobic hydrolysis and anoxic/oxic processes and analysis of bacterial diversity. Bioresource Technology 196, 169-175.

Zhang L., Zhang C., Cheng Z., Yao Y. and Chen J. (2013) Biodegradation of benzene, toluene, ethylbenzene, and o-xylene by the bacterium Mycobacterium cosmeticum byf-4. Chemosphere 90, 1340-1347.